New Horizons in Earth Reinforcement – Otani, Miyata & Mukunoki (eds)
© 2008 Taylor & Francis Group, London, ISBN 978-0-415-45775-0

3D soil reinforcement modeling by means of embedded pile

E.G. Septanika & P.G. Bonnier
Plaxis BV, Delft, The Netherlands

K.J. Bakker & R.B.J. Brinkgreve
Plaxis BV, Delft, Netherlands, Delft University of Technology, Delft, The Netherlands

ABSTRACT: Currently the embedded pile element – consisting of beam elements crossing the soil elements interior, embedded interface to model skin interaction and embedded nonlinear spring to model end capacity – is successfully implemented in the Plaxis 3D Foundation Beta Program. The present embedded pile approach, in which the beam elements can cross the soil element independent of the global mesh structure, makes it also very efficient for modeling large number of piles in e.g. earth reinforcement problem. The interfaces represent both the stiffness and the strength of such pile-soil interaction system. Rigid/flexible connection or inelastic interaction can be modeled by choosing appropriate characteristic of interfaces. For illustration purposes, the 3D modeling capability of the present embedded pile approach is demonstrated by considering slope reinforcement.

1 INTRODUCTION

In the Plaxis 3D Foundation Beta, a so-called embedded pile approach has recently been implemented. Within this approach the pile is assumed as line elements (slender beam elements) instead of volume elements. The slender beam element may have arbitrary inclination and can cross the soil elements at any arbitrary position. The connection between the beam and the soil is established by means of special-purposed interface elements representing the pile-soil contact at the skin and special-purposed non-linear spring representing the pile-soil contact at the base (Septanika, 2005a). In addition to the approach of Sadek and Shahrour (2004), the present embedded pile approach also considers: (i) different types of skin traction/slippage model (constant/linear traction, multi-linear diagram & layer-dependent), and (ii) foot interaction model. Maximum foot resistance is represented by a user-defined maximum value. This value corresponds to the maximum force that can be sustained by the non-linear spring at the pile foot during compression. In case of soil reinforcements, foot interaction is of minor importance.

This paper presents a short description of finite element formulation of the embedded pile approach and it shows the 3D modelling capability of embedded pile in case of slope reinforcement.

2 BACKGROUND

2.1 *Schematization*

The proposed model considers the pile as line elements (i.e. slender beam elements). The beam can cross the bulk soil elements at any arbitrary position and with an arbitrary inclination. Along the axis and at the intersection points between the beam and the soil elements, extra nodes are generated representing the pile nodes.

The displacement of the soil $\mathbf{u}_s$ and of the pile $\mathbf{u}_p$ at any soil-pile contact point $\xi = (\xi, \eta, \zeta)$ follow from the shape functions matrices of the soil element & the pile element and the corresponding nodal displacement vectors of the soil nodes & the pile nodes.

2.2 *Skin interface model*

First the soil-pile contact at the skin/mantle will be described. The soil-pile contact can be represented by a so-called skin traction $\mathbf{t}$ (traction in kN/m = force in kN per circumference in meter). For this purpose, a special-purposed interface element has been developed for connecting the soil element and the pile element. The traction $\mathbf{t}$ at the skin interface is assumed to obey the following constitutive relation

$$\Delta \mathbf{t}^{\text{skin}} = \mathbf{T}^{\text{skin}} \Delta \mathbf{u}_{\text{rel}} \tag{1}$$

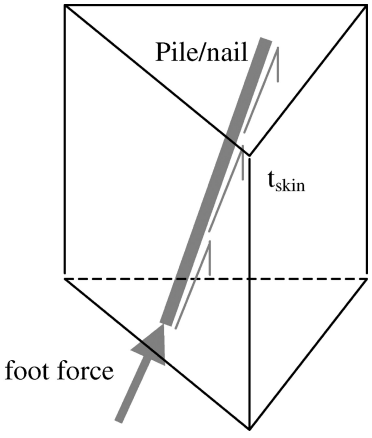

Figure 1. Schematization of a single embedded pile in one soil element.

$$\Delta \mathbf{u}_{rel} = (\Delta \mathbf{u}_p - \Delta \mathbf{u}_s) \tag{2}$$

where $\Delta \mathbf{t}$ is the traction increments at the contact points, $\mathbf{T}^{skin}$ is the material stiffness matrix of the pseudo skin interface and $\Delta \mathbf{u}_{rel} = (\Delta \mathbf{u}_p - \Delta \mathbf{u}_s)$ represents the relative displacement vector between the soil and the pile. The element stiffness matrix $\mathbf{K}_{skin}$ representing the pile-soil interaction at the mantle can be derived based on the following internal virtual work consideration ($\Delta \mathbf{a}$ represents the displacement increments at the corresponding nodes adjacent to the pile skin)

$$\delta(\Delta W^{skin}) = \delta \mathbf{a}^T \mathbf{K}_{skin} \Delta \mathbf{a} \tag{3}$$

where $\mathbf{K}_{skin}$ represents the stiffness contribution of the newly defined pile nodes, the contribution from the soil elements around the pile, and the mixed-terms. Note that since only small displacement differences are desired in the elastic regime, the stiffness of the matrix $\mathbf{T}^{skin}$ should be sufficiently "large" with respect to the bulk soil material. Next, to include slippage at the pile-soil contact, one may limit the shear-traction components. In the current version, the following traction/slippage models are available:

(a) Constant/Linear model relates the allowable traction t_s and the depth y.
(b) Multi-linear diagram by means of a set values of allowable traction values and the corresponding depth (with respect to the pile head); This option can be used to model non-linear skin forces profile which may obtain from pile tests.
(c) Layer-dependent relates the allowable traction with the adjacent soil layer.

Note a rigid connection between pile/reinforcement and the soil can be modeled by assuming very large values of the stiffness components in $\mathbf{K}_{skin}$.

2.3 *Foot interface model*

Next, for the completeness the foot interaction will be also described. The interaction at the foot is modeled by a special-purposed spring element to represent the foot stiffness against the relative movements at the foot. For this purpose, a so-called foot force $\mathbf{F}^{foot}$ vector has been considered obeying the following force-displacement relation

$$\Delta \mathbf{F}^{foot} = \mathbf{D}^{foot} \Delta \mathbf{u}_{rel}^{foot} \tag{4}$$

$$\Delta \mathbf{u}_{rel}^{foot} = (\Delta \mathbf{u}_p - \Delta \mathbf{u}_s) \tag{5}$$

where $\Delta \mathbf{F}^{foot}$ is the force increment at the foot points, $\mathbf{D}^{foot}$ represents the material stiffness matrix of the spring element at the foot, $\Delta \mathbf{u}_{rel}^{foot} = (\Delta \mathbf{u}_p - \Delta \mathbf{u}_s)$ represents the relative displacement vector between the soil and the pile at the foot. By using a similar internal virtual work approach as for the skin interaction the following relations for the foot stiffness matrix $\mathbf{K}_{foot}$ can be obtained ($\Delta \mathbf{a}$ represents the displacement increments at the corresponding nodes adjacent to the pile foot)

$$\delta(\Delta W^{foot}) = \delta \mathbf{a}^T \mathbf{K}_{foot} \Delta \mathbf{a} \tag{6}$$

where $\mathbf{K}_{foot}$ contains the stiffness contribution of the newly defined foot nodes, the contribution from the soil element at the foot, and the mixed-terms. For the maximum foot resistance representing the failure (due to penetration or pulled-out) at the pile foot, the following simplified criterion has been utilized

$$|F_{axial}^{foot}| \le F_{max}^{foot} \quad \text{(for compression)} \tag{7a}$$

$$F_{axial}^{foot} = 0 \quad \text{(for tension)} \tag{7b}$$

where F_{axial}^{foot} is the axial component of the force at the pile foot. In case of reinforcement Eq.(7b) will be valid for both compression and tension.

2.4 *Elastic zone approach*

Embedding the sub-pile/reinforcement to only one adjacent soil element appears to be insufficient and may lead to mesh-dependent behaviour, i.e. the smaller the element, the stronger the local effect. To reduce/eliminate this effect a so-called elastic zone approach has been employed. In this approach all soil points, which fall inside the pile radius (or its equivalent radius), will assume to remain "elastic". This approach appears to be quite robust and sufficient for reducing/eliminating the undesirable mesh-dependent effects (Engin, Septanika and Brinkgreve 2007).

3 NUMERICAL EXAMPLE

The validation of the embedded pile approach in the Plaxis 3D Foundation Beta Program has been presented in previous studies (Septanika 2005a, 2005b; Engin, Septanika and Brinkgreve *et al*. 2007; Septanika, Bonnier, Brinkgreve and Bakker 2007).

3.1 *Previous study on single pile*

3.1.1 *Mesh dependency issue*

Mesh-dependency is highly unpleasant since the total pile capacity may strongly depend on the mesh size. Based on the previous study (Engin, Septanika and Brinkgreve 2007), the application of the elastic zone approach appears sufficient for producing the total pile capacity which is independent of the mesh size. By excluding the elastic zone, the soil elements inside the pile zone will undergo undesirable high inelastic deformation (lowering the capacity). By using the elastic zone mesh independent results are obtained.

3.1.2 *Compression pile test*

To validate the embedded pile for simulating the real case, the Alzey Bridge pile load test (carried out in Frankfurt) has been analyzed. Load cells were I installed at the pile base to measure the loads carried directly by pile base. The layout of the pile load test arrangement is given (El- Mossallamy *et al*. 1997 & 1999). The upper subsoil consist of silt (loam) followed by tertiary sediments down to great depths. These tertiary sediments are stiff plastic clay similar to the so-cal1ed Frankfurt clay, with a varying degree of over-consolidation. It is located completely in the over-consolidated clay. Skin friction curves are obtained by subtracting the base resistance from total load–displacement curve. It was shown that embedded pile model is quite in agreement with the pile load test results (Figure 2). For more details one may refer to Engin, Septanika and Brinkgreve (2007).

3.1.3 *Tension pile test*

The tension tests on bored piles in cemented desert sands (which were carried out in Kuwait) have also been analyzed using the Plaxis 3D Foundation Program. The details of the geometry and soil parameters are given in Ismael *et al*. (1994). The load transfer of bored piles in medium dense cemented sands was investigated by field tests at two sites. The first site (South Surra) has a profile of medium-dense and very-dense weekly cemented calcareous sand. Two short bored piles were tested in axial tension to failure. It was also shown that the total pile capacity according to embedded pile is in reasonably agreement with the results of the tension tests (Figure 3). For more details one may refer to Septanika, Bonnier, Brinkgreve and Bakker (2007).

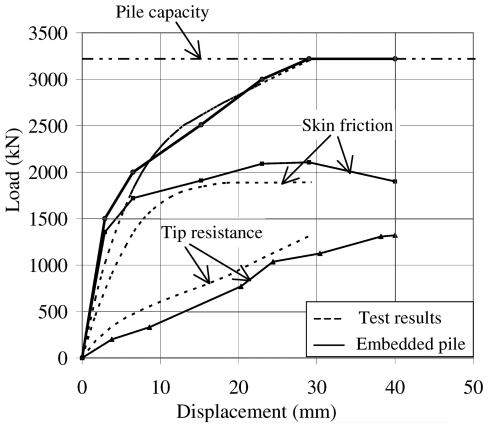

Figure 2. Load-displacement curve of the Alzey bridge pile load test together with Embedded pile results.

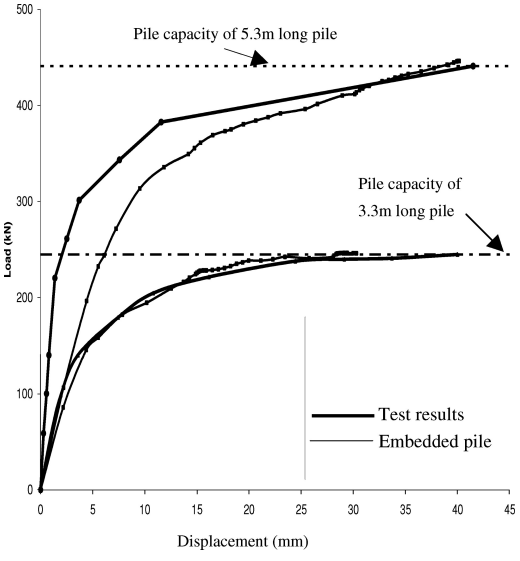

Figure 3. Load-displacement curve of the South Surra pile load test together with Embedded pile results.

3.2 *Pile group application*

For pile grouping application, it is possible to generate a 3D finite element model in which the piles can be inclined with respect to the vertical axes. Without mentioning further details, the Figure 4 below shows a raft foundation of a building supported by inclined piles. It can be seen that the mesh structure of the soil is not affected by existence of the inclined piles. The interaction between the pile and soil is realized, firstly by taking into account for the pile stiffness (also including the elastic zone of each pile) that reinforces the adjacent soil, and secondly a proper modeling of skin

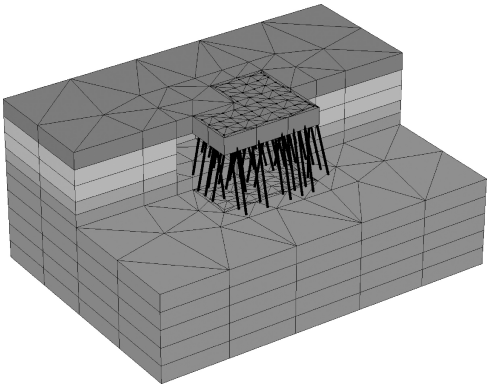

Figure 4. 3D-model of pile raft foundation using embedded piles.

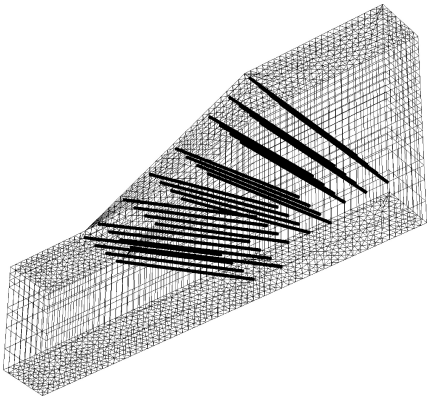

Figure 5. 3D finite element modeling of reinforced slope using embedded piles.

and foot resistances defines the strength of the pile-soil connection. Note that when using volume piles, each pile is modeled by means of a number of volume elements that leads to huge small soil element around the piles and a complex 3D mesh structure due to pile inclination and different soil layers.

3.3 *Reinforcement of slope*

For illustration purposes the application of embedded pile as reinforcements in a reinforced slope problem has been considered (Figure 5). This numerical example shows the 3D modeling capability of embedded pile approach in the Plaxis 3D Foundation Program. Due to the existence of nails – modeled by means of inclined embedded (micro) pile – the slope increases its stiffness. In contrast to the classical reinforcement approach in which the reinforcement is rigidly connected to the soil elements, the strength of the present

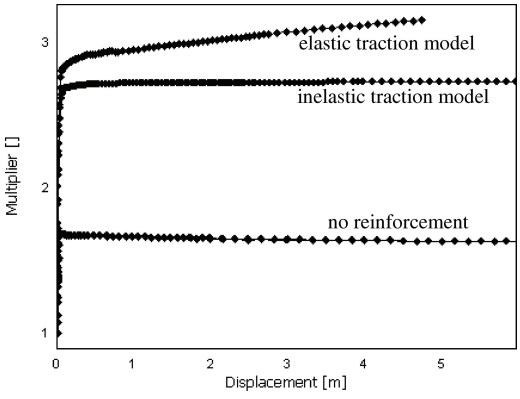

Figure 6. Safety analysis of the slope stability problem using elastic & inelastic skin traction model at embedded pile.

type of nailing element can be limited by a user-defined maximum value of shearing traction/force along the pile skin. Rigid connection is simply modeled by using very high stiffness and very high maximum value of shearing traction/force, while a more realistic traction limit value can be obtained from e.g. pull-out tests.

For the present analysis a slope of 10 m high has been considered (with inclination of around 45° with respect to the horizontal axis). The soil behaviour is according to the Mohr-Coulomb model with the following parameters: Young's modulus $E = 2.10^4$ kPa, Poisson's ratio $\nu = 0.3$, cohesion $c = 10$ kPa, friction angle $\varphi = 30°$. The result of safety analyses of the reinforced slope using embedded pile model in Plaxis 3D Foundation Beta program is shown in Figure 6. It is show that the slope with no reinforcement has a lower factor of safety FS as compared to the reinforced soil (i.e. employing the phi-c method). Two cases have been considered: (i) based on inelastic skin traction model by presuming a certain skin traction limit, (ii) based on the "elastic" model using a very large value of skin traction limit. Note that the elastic model is comparable to reinforced soil, excluding the relative movements between soil and the reinforcements. It can be seen that the elastic traction model leads to an (unrealistic) overestimated behaviour. The results also show the usefulness of the present inelastic skin traction option in modelling the failure behaviour of reinforced slope.

Further, the total deformation mechanism in case of no reinforcements and reinforced slope are shown in Figure 7 and Figure 8. The axial force distribution and the skin traction distribution for a typical reinforcement are shown in Figure 9(a)–(b). It has to be note that the present results are based on a simplified inelastic traction model and are purposed for demonstration

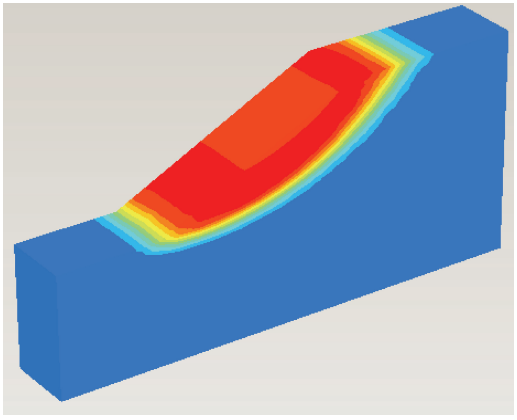

Figure 7. Deformation mechanism in case of no reinforcements.

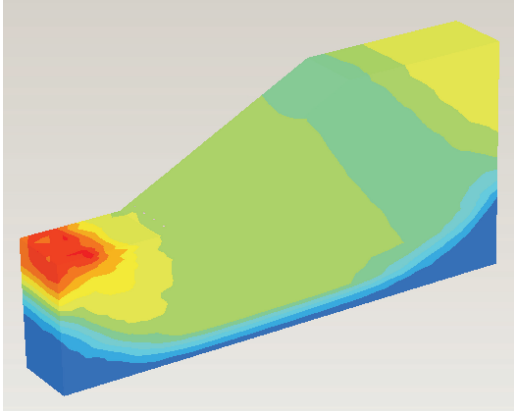

Figure 8. Deformation mechanism in case of reinforced slope.

only. More realistic skin traction distribution can be estimated by using advanced inelastic skin traction models, based on more accurate soil data and pull-out test data.

4 CONCLUDING REMARKS

This paper shortly describes the embedded pile approach, followed by a review of validation tests that have been done previously. The accuracy of single pile model has been validated, by considering the pile compression tests in Frankfurt and the pile tension tests in Kuwait. For both cases, the results are reasonably in agreement with the field test results. It is important to mention that an accurate modelling of the soil part also plays an important role for simulating the behaviour

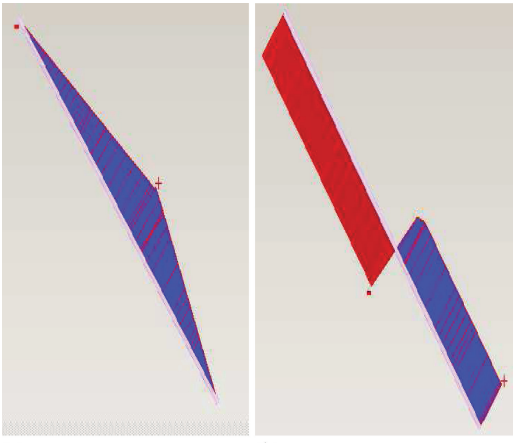

(a) (b)

Figure 9. (a) Axial force distribution at the reinforcement, (b) Skin traction distribution at the reinforcement.

of the real tests. With the embedded pile approach it has been shown that 3D modelling of multi piles application (with or without inclination) can be relatively easy generated. The resulting 3D mesh structure is unaffected by the existence of the pile. Finally, a reinforced slope problem has been considered to illustrate the modelling capability of the present embedded pile in the Plaxis 3D Foundation Program. It was shown that the factor of safety FS in the reinforced slope is much higher than without the reinforcement. In the near future more study will be performed concerning to further evaluate the capability of embedded pile in pile group applications and soil reinforcement problems.

REFERENCES

El-Mossallamy, Y. and Franke, E. (1997). Numerical Modelling to Simulate the Behaviour of Piled Raft Foundations, August 1997, Darmstadt, Germany.

El-Mossallamy, Y. (1999). Load-settlement behaviour of large diameter bored piles in over-consolidated clay. *Proc. of the 7th intern. symp. on numerical models in geotechnical engineering* – NUMOG VII, Graz, 1–3 September 1999, 443–450. Rotterdam: Balkema.

Engin, H.K., Septanika, E.G. and Brinkgreve, R.B.J. (2007). Improved embedded beam elements for the modelling of piles. *International Symposium on Numerical Models in Geomechanics* – NUMOG X, Rhodes, Greece. April 2007.

Ismael, N.F., Al-Sanad, H.A. and Al-Otaibi, F. (1994). Tension tests on bored piles in cemented desert sands. *Canadian Geotechnical Journal*, Vol. 31 (4), 597–603.

Sadek, M. and Shahrour, I. (2004). A three dimensional embedded beam element for reinforced geomaterials. *International journal for numerical and analytical methods in geomechanics* 28:931–946.

Septanika, E. G. (2005a). A finite element description of the embedded pile model. Plaxis internal report.

Septanika, E. G. (2005b). Validation testing embedded pile in Plaxis 3D Foundation. Plaxis internal report.

Septanika, E.G., Bonnier, P.G., Brinkgreve, R.B.J. and Bakker, K.J. (2007). An efficient 3D modelling of (multi) pile-soil interaction. *Proceeding of Third International Geomechanics Conference*, 11–15 June 2007, Nessebar, Bulgaria.

Skempton, A.W. (1951). The Bearing Capacity of Clays. *Proceeding of Building Research Congress*, Vol. 1, 180–189.